Polymer Chemistry

RSC Publishing

PAPER

View Article Online
View Journal | View Issue

Cite this: *Polym. Chem.*, 2013, **4**, 1482

Block copolymer supramolecular assembly using a precursor to a novel conjugated polymer†

Daniel Hagaman,[a] Jacob Gredzik,[a] Patricia A. Peart,‡[b] J. Michael McCaffery,[c] John D. Tovar[b] and Alexander Sidorenko*[a]

Received 24th August 2012
Accepted 29th November 2012

DOI: 10.1039/c2py20680c

www.rsc.org/polymers

Block copolymer supramolecular assemblies (SMAs) have been used to prepare nanotemplates and nanoarrays of a variety of materials. This has been achieved *via* selective H-bonds between a low molecular weight additive and one block of the block copolymer. Herein we propose to extend the range of the additives by exploring multiple weak interactions other than hydrogen bonding. This is illustrated with the following SMA: diblock copolymer poly(styrene-*b*-4-vinylpyridine) (PS-*b*-P4VP) and the low molecular weight additive 1,5-bis(2,3-dihydrothieno[3,4-*b*][1,4]dioxin-5-yl)-1,6-methano[10]annulene (bisEDOT), a molecule synthesized specifically for this project. Through rational design, bisEDOT possesses several characteristics which make it a suitable candidate for functional SMA formed without hydrogen bonds. It has multiple sites for SMA formation, exhibits photoluminescence, and is a precursor to an electroconductive polymer. Also, removal of bisEDOT results in porous thin films allowing us to study the morphology using AFM. C-AFM confirms that polymerization of bisEDOT leads to electroconductive polymer thin films. In this work, we discuss the formation of this SMA as well as *in situ* polymerization of bisEDOT in SMA thin films.

Introduction

A single molecule of a block copolymer (BCP) is comprised of two (diblock) or more chemically different polymer chains. In such a molecule, the polymer chains are covalently bound together. Typically, the polymer subunits individually are immiscible, and when mixed they undergo phase separation. The phase separation in BCP, however, occurs on the micro-scale due to the covalent bond between the different chains. This microphase separation produces well-defined morphologies on the nanometer (nm) length scale, usually between 10 and 100 nm.[1] Thermodynamically, microphase separation in BCPs is driven by the interfacial energy between the morphological features as well as the entropy caused by chain stretching.[2] The morphology a BCP adopts also depends on the Flory–Huggins interaction parameter χ, volume fraction f, and the degree of polymerization N of each block. An A–B diblock copolymer with a 50 : 50 volume fraction among the two components exhibits the lamellar morphology. As the volume fraction of one block decreases the following morphologies are observed: bicontinuous gyroid, hexagonally packed (HEX) cylinders, and body-centered cubic (BCC) spheres.[3]

Recently, the group led by O. Ikkala has developed a new class of materials which combine BCP and a low molecular weight additive. They are commonly referred to as comb-like polymers[4] or block copolymer supramolecular assemblies (SMAs).[5] The SMAs consist of a BCP and a low molecular weight additive that selectively associates with one block of the BCP. In most cases, hydrogen bonding governs the formation of an SMA. An example of hydrogen bonded SMA is between the BCP poly(styrene-*b*-4-vinylpyridine) (PS-P4VP) and the additive *n*-pentadecylphenol (PDP). The SMA is formed through a hydrogen bond between the nitrogen on pyridine and the hydroxyl group of PDP. Other examples of additives include 2-(4′-hydroxybenzeneazo)-benzoic acid (HABA),[5,6] octylgallate,[7,8] 1-pyrenebutyric acid,[9] resorcinol,[10] carbohydrates,[11] 1,5-dihydroxynaphthalene,[12] and quarterthiophene.[13] Besides small molecules, mixtures of BCPs with homopolymers of one block can exhibit similar properties to that of an SMA due to the association of the homopolymer within a BCP domain.[14] Regardless of the additive, the parent BCP and its corresponding SMA have very different properties. Besides the quantitative difference due to the selective increase of volume fraction, tuning the BCP : additive molar ratio can result in a variety of morphologies not available to the parent BCP.[4–6] Also, the incorporation of an additive within a BCP domain causes microphase separation to occur faster relative to the parent BCP

[a]*Department of Chemistry and Biochemistry, University of the Sciences, Philadelphia, PA 19104, USA. E-mail: a.sidorenko@usciences.edu; Tel: +1 (215) 596 8836*

[b]*Department of Chemistry, Johns Hopkins University, Baltimore, MD 21218, USA*

[c]*Integrated Imaging Center, Department of Biology, Johns Hopkins University, Baltimore, MD 21218, USA*

† Electronic supplementary information (ESI) available. See DOI: 10.1039/c2py20680c

‡ Current address: Senior Chemist, The Dow Chemical Company, Midland, MI 48674, USA.

which can result in an improved overall order. In an SMA, additives can also interact with themselves. This may result in hierarchical morphologies which are observed due to the organization of the additive within a domain. This small length scale ordering is also referred to as "structure-within-structure" morphology. These morphologies were first observed by Ruokolainen *et al.* in the PDP-SMA.[15] Besides changes in morphology further manipulation of SMAs is possible. Because SMAs are formed through non-covalent bonding, the additive can be dissolved and extracted with a selective solvent from both bulk and thin films without compromising the integrity of the remaining BCP films.

When the additive is removed, it leaves a mesoporous BCP template. Such nanotemplates can be used for the formation of functional materials inside the empty domains. Examples using inorganic materials include quantum dots[16] and various metals such as nickel, palladium, gold and platinum.[5,17,18]

The past two decades have seen a significant amount of research in the area of polymer/organic photovoltaic and light emitting devices because of the need for an alternative to the inorganic semiconductors traditionally used. Intrinsically conducting polymers have been recognized as a material with the potential to replace inorganic semiconductors for low-cost and large-area flexible applications in order to help meet the need of society's growing energy demand.[19] Devices such as solar cells, organic field effect transistors (OFETs), and organic light emitting diodes (OLEDs) are just a few examples of where these materials can be substitutes for conventional semiconductors. While electroconductive polymers have found many applications, some inherent drawbacks still remain. Due to the conjugated backbone, they exhibit poor solubility which leads to intricacies in preparing thin films.[20] Preparation of these materials with nanostructures could be an option that would improve and expand the capabilities of organic electronics while enabling large-scale processing. The "bottom up" approach to achieve nanomaterials uses the self-assembly of BCPs. Recently, Kuila *et al.* have combined these two technologies by electrochemical synthesis of polyaniline in nanotemplates made from an SMA containing PS-*b*-P4VP and HABA.[21]

The SMA discussed in this paper goes beyond hydrogen bonding (HB) and relies on a combination of other weak intermolecular interactions to achieve SMA formation. Recently, we have proved the viability of the non-HB approach to SMA using several additives of the thiophene family, *i.e.* 3,4-ethylenedioxythiophene (EDOT) and 3,4-(2,2-dimethylpropylenedioxy) thiophene.[22] Here we present a novel SMA (bisEDOT-SMA) composed of the poly(styrene-*block*-4-vinyl pyridine) parent BCP and 1,5-bis(2,3-dihydrothieno[3,4-*b*][1,4]dioxin-5-yl)-1,6-methano [10]annulene (bisEDOT), *i.e.* a methano[10]annulene molecule substituted with EDOT in positions 2 and 7, as the soluble low molecular weight additive (Fig. 1). Methano[10]annulene is a non-traditional aromatic molecule initially synthesized by Vogel and Roth.[23] As opposed to the traditional planar aromatics (the closest analogue is naphthalene), the molecules of methano[10] annulene and the substituted derivatives are non-planar and racemic, revealing numerous interesting properties.[24] BisEDOT is particularly interesting as an additive for the SMA. Unlike most additives used in SMAs, bisEDOT plays multiple roles as it is used for the formation of the SMA with a specific morphology while also being a fluorescent marker and a precursor to an electroconductive polymer. In this article we will show that this type of

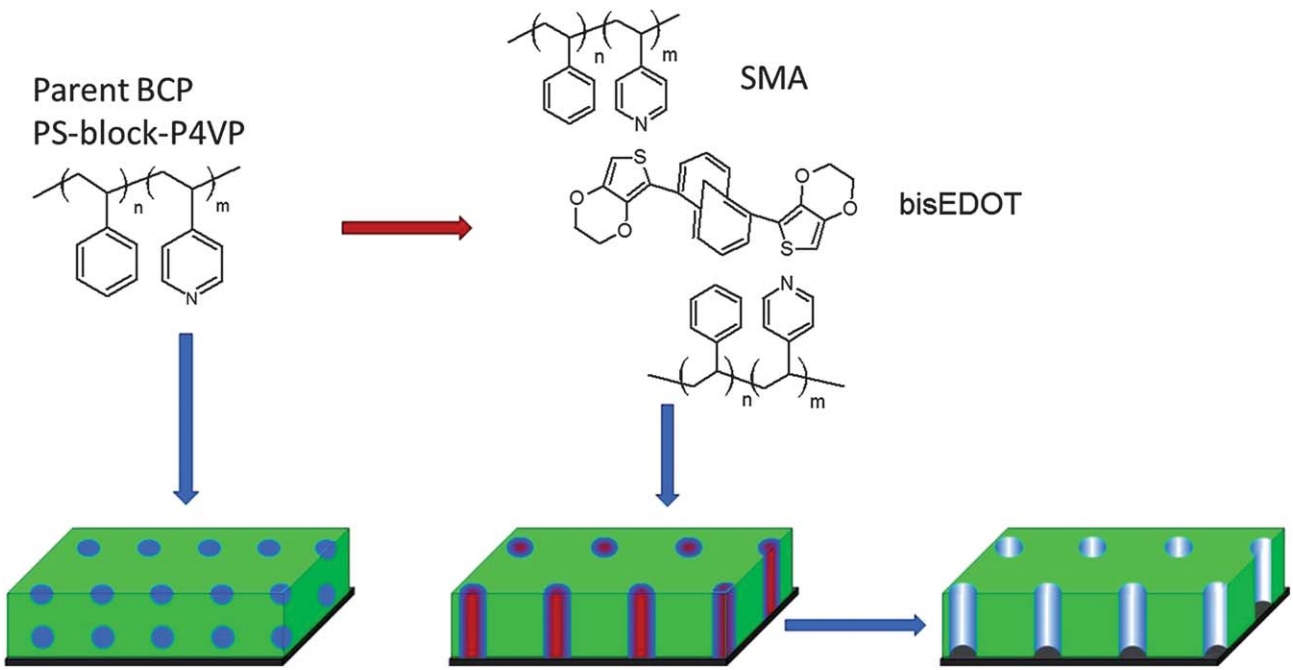

Fig. 1 Concept of the bisEDOT-SMA formation and corresponding morphology evolutions: spherical BCC morphology of parent BCP (left), perpendicular cylindrical morphology of SMA (center), and porous BCP film upon extraction of the additive (right).

SMA may lead to functional nanomaterials by *in situ* polymerization of bisEDOT-SMA thin films.

Experimental

Materials

Poly(styrene-*block*-4-vinylpyridine) (PS-*b*-P4VP), with a number averaged molecular mass (M_n) of PS 35 500 g mol^{-1}, P4VP 4400 g mol^{-1}, $M_w/M_n = 1.09$ for both blocks, was purchased from Polymer Source, Inc. Solvents chloroform, dichloromethane, 1,4-dioxane, methanol and dimethylformamide (DMF) were purchased from Sigma-Aldrich. DMF was degassed by purging with argon, and all other solvents were used as received. Tetrakis(triphenylphosphine)palladium, $Pd(PPh_3)_4$, was obtained from Strem Chemicals. *N*-Bromosuccinimide, 3,4-ethylenedioxythiophene, and tributylstannylchloride were obtained from Sigma-Aldrich or Bayer. All other chemicals were obtained from Sigma-Aldrich and used without further purification. Silicon wafers ⟨100⟩ were cleaned successively in an ultrasonic bath (dichloromethane, methanol, millipore water) for 15 min and then in a 2 : 1 : 1 alkali "piranha" solution (H_2O–H_2O_2–NH_4OH) at a temperature of approximately 80 °C for 1 h. The wafers were then rinsed thoroughly with millipore water and dried under an argon flow.

UV-visible spectroscopy

A Varian Cary 100 Bio Spectrophotometer was used to collect UV-vis spectra of the SMA. The spectra were obtained in the solution using 1,4-dioxane as the solvent or as thin films deposited on glass slides.

Photoluminescence spectroscopy

Spectra were obtained on a Photon Technology International (PTI) fluorimeter equipped with a Xenon arc lamp and a PMT detector. Excitation spectra were collected between 200 and 510 nm at an emission wavelength of 520 nm. Emission spectra were obtained between 400 and 700 nm. The excitation wavelength for bisEDOT was 385 nm. Excitation wavelengths for bisEDOT-SMA were 350 and 415 nm. Spectra were obtained at room temperature. The solvent used for all solutions was 1,4-dioxane.

Spectroscopic ellipsometry

Both thickness and porosity of thin SMA films were measured using a spectroscopic ellipsometer PhE 102 (Angstrom Advanced Inc.). Measurements were taken at an incident angle of 70° in the wavelength range of 350 to 800 nm. A standard model of Si/SiO_2/polymer was employed. The porosity was estimated with the Effective Medium Approximation (EMA).

Atomic force microscopy

Atomic force microscopy (AFM) images were obtained using a diInnova (Veeco) scanning probe microscope in tapping mode. The AFM probes (Budget Sensors) used have the following features: a resonant frequency of 190 kHz and a spring constant of 48 N m^{-1}. Any measurement taken from an AFM image was carried out using WSxM software (Nanotec Electronica).[25]

Conductive AFM measurements (C-AFM) were taken using a Multimode Picoforce SPM (Veeco) equipped with a Nanoscope V controller and C-AFM module. The C-AFM probes (NanoWorld) used had a Pt/Ir coating (both sides), a resonance frequency of 13 kHz, and a force constant of 0.2 N m^{-1}.

Synthesis of bisEDOT

All reactions were performed in flame-dried glassware which had been cooled under nitrogen. The reactions were carried out under an atmosphere of nitrogen. 2,7-Dibromo-1,6-methano [10]annulene was prepared by brominating methano[10]annulene with *N*-bromosuccinimide.[26] 2-Tributylstannyl-3,4-ethylenedioxythiophene was synthesized by first lithiating 3,4-ethylenedioxythiophene and quenching with tributylstannylchloride.[27] ^{1}H-NMR and ^{13}C-NMR spectra were obtained for samples in deuterated chloroform (peak set at 7.26 ppm for ^{1}H-NMR and 77 ppm for ^{13}C-NMR) using a Bruker Avance 400 MHz FT-NMR spectrometer. Mass spectra were obtained using a VG Instruments VG70S magnetic sector mass spectrometer, with EI and CI ionization.

1,5-Bis(2,3-dihydrothieno[3,4-*b*][1,4]dioxin-5-yl)-1,6-methano [10]annulene (bisEDOT)

To a 25 mL Schlenk tube was added 2,7-dibromo-1,6-methano [10]annulene (199 mg, 0.66 mmol) and $Pd(PPh_3)_4$ (36 mg, 0.03 mmol). The vessel was evacuated and placed under nitrogen. DMF (5 mL) was added and the mixture was stirred to dissolve the solids. 2-Tributylstannyl ethylenedioxythiophene (604 mg, 1.40 mmol) was added and the solution was heated to 80 °C and left to stir for 36 h during which time the solution turned black. The reaction was allowed to cool to room temperature at which point the solution was diluted with ether (20 mL) and stirred vigorously with the added 1 M KF solution (40 mL). The aqueous layer was removed and the organic layer was washed with a 1 M KF solution (40 mL) and NH_4Cl (2 × 50 mL). The organic phase was dried over $MgSO_4$, filtered and evaporated under reduced pressure. The product was further purified on a silica gel column using 1 : 1 hexane/DCM (with 5% triethylamine) as the eluent to yield bisEDOT (185 mg, 0.44 mmol, 66%) as yellow crystals. ^{1}H-NMR (400 MHz, $CDCl_3$) δ: 7.66 (d, $J = 8$ Hz, 2H), 7.35 (d, $J = 8$ Hz, 2H), 7.12 (t, $J = 8$ Hz, 2H), 6.40 (s, 2H), 4.30 (m, 8H), −0.08 (s, 2H). ^{13}C-NMR (100 MHz, $CDCl_3$) δ: 141.9, 137.7, 131.7, 127.7, 127.2, 117.4, 116.9, 100.1. HRMS (EI) calculated for $C_{23}H_{18}O_4S_2[M^+]$: 422.0647. Found: 422.0642.

Preparation of SMAs

PS-*b*-P4VP and bisEDOT were dissolved separately in 1,4-dioxane. The PS-*b*-P4VP solution was added dropwise to the bisEDOT solution while it was sonicated and heated (40 °C) simultaneously. BisEDOT and P4VP were in a 1 : 2 molar ratio, respectively. This molar ratio was used because one bisEDOT molecule is capable of interacting with two molecules of pyridine. The bisEDOT-SMA solution was aged at least one month before use to establish equilibrium and complete its formation.

Prior to use, all solutions were filtered using 0.2 μm pore size PTFE filters. Thin films were deposited directly from the bisEDOT-SMA solution onto clean silicon wafers. They were deposited by either dip-coating or spin-coating technique. The deposition conditions were maintained to produce films with thicknesses of 50 to 80 nm unless otherwise stated.

Results and discussion

Synthesis of bisEDOT

With the great results that have been obtained employing poly(3,4-ethylenedioxythiophene) (PEDOT) as an electroconductive polymer, it is no surprise that much work has been done incorporating EDOT into conductive organic polymers. One way in which this can be achieved is to make oligomers consisting of EDOT and an aryl group. These may subsequently be used as monomers in the synthesis of conductive polymers. For example, Reynolds *et al.* have synthesized and characterized a series of EDOT containing monomers.[28] These include 2,5-bis(ethylene-dioxythiophenyl)thiophene, 2,5-bis(ethylene-dioxythiophenyl)furan, 1,4-bis-(ethylene-dioxythiophenyl)benzene, 3,4-ethylenedioxythiophene, 4,4′-bis(ethylenedioxy-thiophenyl) biphenyl and (*E*)-1,2-bis(ethylenedioxythiophenyl)vinylene. One of the ideas behind their work is that having these three-ring monomers would increase conjugation thereby forming a monomer with a low oxidation potential. As such, EDOT itself already possesses a low monomer oxidation potential and has been thought to be the perfect candidate for the end rings. The reported monomer oxidation potentials range from 0.20–0.75 V and band gaps range from 1.4 to 2.3 eV. The lowest values reveal 3,4-ethylenedioxythiophene which may be the most easily polymerized thiophene-based polymer.[25] The polymers formed from these monomers exhibit a range of colour changes that vary with applied electrochemical potential indicating that they may be used as electrochromic materials. We thus have synthesized bisEDOT *via* Stille coupling of 2-tributylstannyl-3,4-ethylenedioxythiophene with 2,7-dibromo-1,6-methano[10]annulene (Fig. 2). BisEDOT has many favourable properties for use as an additive in SMA. First, the two EDOT groups make it an ideal choice because they can form multiple interactions with P4VP. These interactions are the driving force of SMA formation. Second, it is a polymerizable precursor to a π-conjugated polymer, making it a functional material with potential applications in organic electronics. Third, the non-planar and racemic nature of the bisEDOT monomer should offer greater solubility in the SMA solutions relative to more crystalline planar variants. Driven by this rationale, we expected bisEDOT to be suitable for the non-HB functional SMA.

After some investigation, other benefits were soon discovered. The bisEDOT-SMA is easily characterized in the solution by simple spectroscopy techniques such as photoluminescence and UV-vis. BisEDOT is also readily soluble in 1,4-dioxane which is the solvent used for our SMA solutions. The preliminary experiments have shown that non-HB SMAs are very sensitive to solvent properties. The solvent should be able to dissolve the BCP and additive, but not prevent the formation of new interactions between the two. Lastly, because of the extended conjugation present in the molecule due to the bridging 1,6-methano[10]annulene group, this molecule has a low oxidation potential.[29,30] The low oxidation potential is an advantage for the *in situ* polymerization of bisEDOT in bisEDOT-SMA thin films.

UV-visible spectroscopy

UV-vis spectroscopy was employed to investigate the properties of both pure bisEDOT and the bisEDOT-SMA. Spectra of thin films of 100 nm in thickness were obtained by depositing the bisEDOT-SMA on cleaned quartz glass slides. The solution of pure bisEDOT in 1,4-dioxane reveals two absorption bands, 291 and 385 nm (Fig. 3). The band at 385 nm is of interest because it exhibits fluorescence and also is responsible for the bright yellow colour of solutions and thin films (on glass). The spectrum of the bisEDOT-SMA solution (Fig. 3, solid) shows no difference from the pure bisEDOT spectrum. However, the spectrum of the bisEDOT-SMA thin film is different from that of

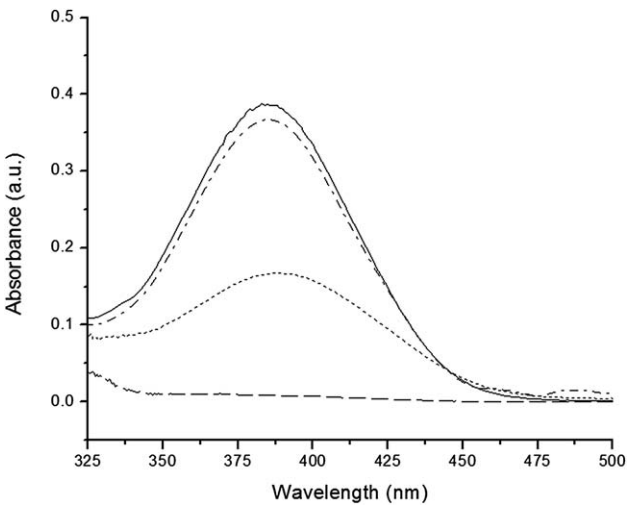

Fig. 3 UV-visible spectra of the bisEDOT-SMA solution (solid), bisEDOT solution (dash dot), bisEDOT-SMA thin film (dots), and bisEDOT-SMA thin film after washing in methanol (dash).

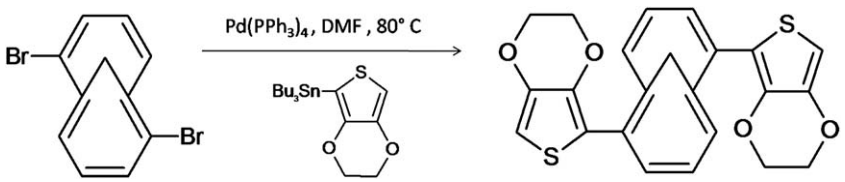

Fig. 2 Synthesis of bisEDOT *via* Stille coupling of 2-tributylstannyl-3,4-ethylenedioxythiophene and 2,7-dibromo-1,6-methano[10]annulene.

the pure bisEDOT solution (Fig. 3, dots). The peak at 385 nm is slightly red-shifted to 390 nm. After examining the thin film with AFM and detecting no signs of phase separation (crystals or other features), we attribute this red-shift to the aggregation of bisEDOT within the P4VP domains. This shift to lower energy is usually associated with J-aggregation.[31,32] However, with only a 5 nm difference we are inclined to attribute this shift to a more planar conformation of bisEDOT induced by interactions with P4VP in bisEDOT-SMA thin films. UV-vis spectroscopy also allows us to monitor the removal of bisEDOT from thin films with methanol which is a selective solvent. Being soluble in methanol, bisEDOT is completely removed, leaving a porous BCP thin film. The voids are formed by the extracted additive while the BCP matrix remains intact. The removal of bisEDOT from the thin film is confirmed by the disappearance of the absorption band at 385 nm (Fig. 3, dash).

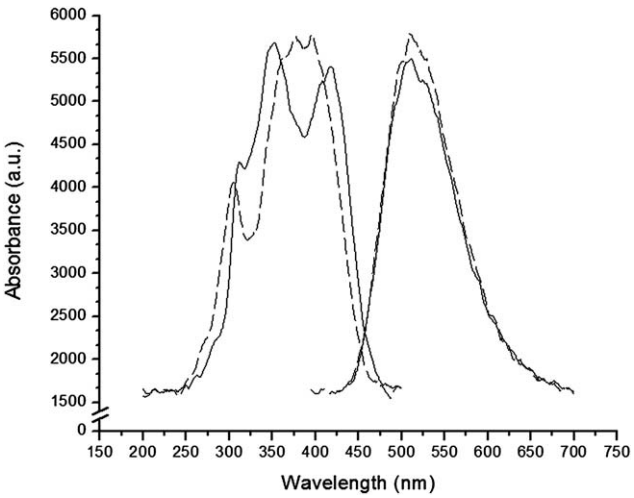

Fig. 4 Excitation and emission spectra of bisEDOT and bisEDOT-SMA solutions. Spectra were collected at room temperature. The emission wavelength for both bisEDOT (---) and bisEDOT-SMA (—) was 520 nm. The excitation wavelength for bisEDOT (---) was 385 nm. Excitation wavelengths for bisEDOT-SMA (—) are 350 nm and 415 nm.

Photoluminescence spectroscopy

For HB-based SMAs, FT-IR has been previously employed to detect the formation of hydrogen bonds for the purpose of confirming SMA formation and investigation of fine intermolecular interactions. One example is the analysis of the comb shaped polymer formed by a HB between the homopolymer P4VP and the additive PDP.[33] Similarly, the details of interactions caused by different solvents have been revealed in the HABA-SMA.[4,5] Here, the weaker Lewis acid–base or donor–acceptor interactions are employed to form the non-HB SMA. We have previously shown that interactions between the additive and the parent BCP in non-HB SMA are inactive in the IR range.[22] Instead, we chose photoluminescence (PL) spectroscopy to study the bisEDOT-SMA. PL spectra were obtained for pure bisEDOT and the bisEDOT-SMA in the solution. PL spectroscopy is useful because in addition to information about electronic transitions for bisEDOT, we can gain insight into its local environment. This is especially important for the bisEDOT-SMA as it may prove new interactions between bisEDOT and P4VP resulting in a SMA.

The PL spectrum for pure bisEDOT shows an excitation peak at 385 nm with emission at 520 nm. In contrast, the excitation spectrum of the bisEDOT-SMA solution reveals two separate and narrower peaks at 350 and 415 nm in the place of the original broad peak at 385 nm (Fig. 4). For the bisEDOT-SMA the emission peaks remain unchanged in both position and shape whether the excitation peak used was 350 or 415 nm. We attribute the differences in the vibronic features in the excitation spectra to the reduced amount of torsional freedom available to the bisEDOT monomers when confined by the local environment of the SMA.

Thin film characterization

The microphase separation in a BCP results in a number of discrete morphologies which have features on the nanometer length scale. The extraction of an additive with a selective solvent usually results in porous films.[4,5,31] This makes AFM an ideal tool for investigating thin films of BCP to reveal their surface morphology as well as a quantitative assessment of their features. Thin films differ from the bulk because their thickness (*z*-dimension) is on a different length scale (usually nm) than their lateral dimensions (at least mm). Because the film thickness is on the same length scale as the features of the morphology, their orientation can be defined. For morphologies such as cylinders and lamellae, the orientation of the morphology relative to the substrate can be either perpendicular or parallel.[5]

Using AFM, we compared the resulting morphologies of our bisEDOT-SMA to the parent PS-*b*-P4VP BCP. Thin films of neat PS-*b*-P4VP showed hexagonally ordered spherical domains of P4VP in a BCC lattice. The minor component of our block copolymer (P4VP) has a volume fraction of approximately 0.10 which is consistent with this spherical morphology. The Power Spectral Density analysis and FFT calculation of the AFM topography image reveals the periodicity of the spheres to be 23 nm. With this measurement as a baseline, all bisEDOT-SMA thin film measurements are compared to this number. A selective interaction between the additive and one block of the BCP is a requirement for SMA formation. In our case, bisEDOT and P4VP interact to form a new block both in the solution (as revealed by fluorescence) and in thin films. Assuming a full association between bisEDOT and P4VP, the volume fraction of the minor block would increase to approximately 0.25. In most cases for diblock copolymers, this volume fraction corresponds to hexagonally packed cylinders. To start, we investigated as-deposited thin films of bisEDOT-SMA. The films were smooth and usually no fine structure with light tapping mode was observed. After extraction of bisEDOT with methanol, poorly ordered wells were observed (Fig. 5). These features could indicate either spheres or cylinders without any particular orientation. A FFT reveals a periodicity of 27 nm for this image. This increase in periodicity of the features leads us to believe that the quasi-hexagonally ordered structures are cylinders, and

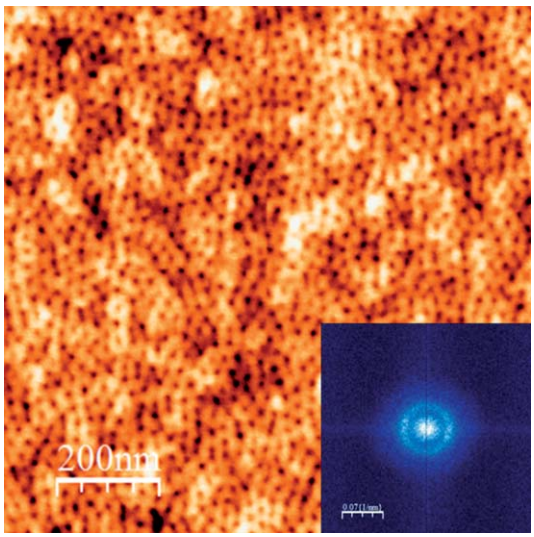

Fig. 5 A 1 × 1 μm topography image of an as-deposited bisEDOT-SMA thin film, 60 nm in thickness. Inset is the corresponding 2D-FFT.

not spheres. Based on the results of similar SMA with HABA and EDOT-family additives obtained with the same or similar parent BCP, such increase is significant to prove the cylinder formation.[4,5,31] However, because bisEDOT is capable of interacting with two pyridine molecules, one may expect rather efficient packing within the P4VP domains.

Extraction of bisEDOT should result in porous films. We have evaluated the porosity of the films using ellipsometry. A 100 nm thick bisEDOT-SMA film showed a minor decrease in thickness upon extraction of bisEDOT resulting in 0.171 porosity using a linear EMA model (see ESI†). Assuming the equal density of bisEDOT and the polymer matrix, the theoretical porosity based on mass balance of the components was calculated to be 0.181. Hence, ellipsometry proves successful and complete extraction of the additive in bisEDOT-SMA.

To confirm that the hexagonal structures in the SMA thin films were cylinders, we performed vapour annealing to switch the orientation of the morphology from perpendicular to parallel. Vapour annealing has been proved to be a useful technique to control the orientation of thin films and to improve overall ordering. In the case of the SMA between PS-*b*-P4VP and HABA, annealing with vapours of chloroform was shown to rearrange perpendicular cylinders to the parallel orientation.[5]

Annealing the thin films of the bisEDOT-SMA in vapors of 1,4-dioxane, a selective (preferential) solvent for the major component of the BCP, results in improved ordering and perpendicular orientation of the cylinders (Fig. 6a). There are no significant changes in the periodicity for thin films annealed in 1,4-dioxane, though. Obtaining the parallel orientation in bisEDOT-SMA thin films is not a straightforward task. Annealing in a non-selective solvent such as chloroform does not result in the parallel orientation as it did for the HABA-SMA. The interactions between bisEDOT and pyridine are interrupted during annealing when using a strong electron-acceptor solvent such as chloroform. This results in macrophase separation of

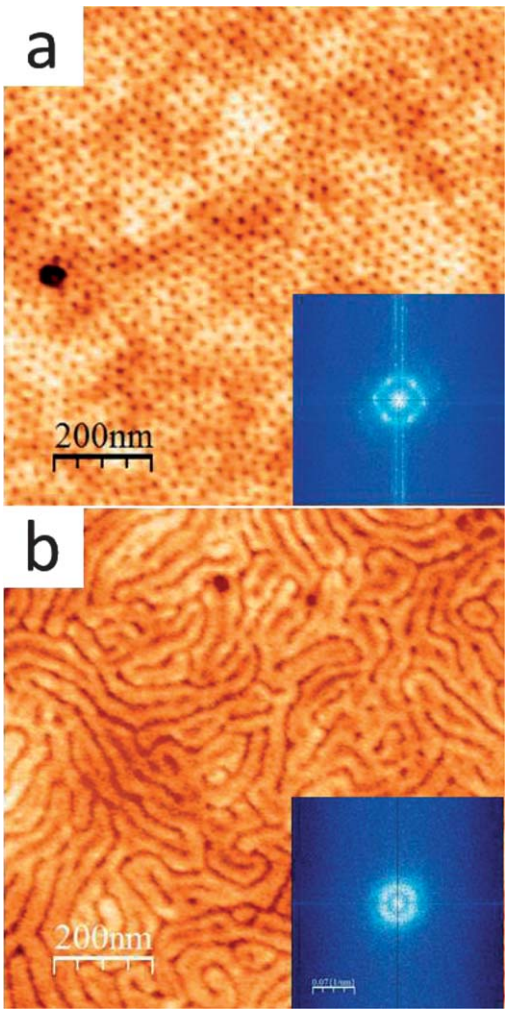

Fig. 6 1 × 1 μm topography images of bisEDOT-SMA thin films vapor annealed in 1,4-dioxane (a) and toluene–methanol (50/50 wt%) (b). Insets are corresponding 2D-FFT images. Thickness of both films is 60 nm.

the additive. This challenge was overcome by using a binary solvent system to create a non-selective solvent that did not affect the interactions in our bisEDOT-SMA. Vapor annealing of BCP thin films with solvent mixtures has been reported previously. Recently, the morphology transitions of the BCP poly(styrene-*b*-isoprene-*b*-styrene) were studied after vapor annealing in *n*-hexane–THF mixtures.[34] Equally successful were studies of the effect of the solvent parameter on morphology and the structure of PS-*block*-P4VP films.[35] To meet our needs, the solvent system chosen was a mixture of toluene and methanol. Fig. 6b shows the result of annealing a bisEDOT-SMA thin film in vapors of a 50/50 wt% toluene–methanol solution. The Power Spectral Density analysis of the image in Fig. 6b gives the periodicity of 39 ± 2 nm for the parallel cylinders. This confirms our previous assumption that the hexagonally ordered features observed in as deposited bisEDOT-SMA thin films are cylinders.

Within the range of probed thicknesses of 50 to 100 nm we have observed poorly ordered quasi-hexagonal surface patterns which correspond to cylindrical morphology. Additional probing of the SMA morphology was done using cross-sectional TEM (ESI†).

In situ polymerization

We explored the capability of bisEDOT for oxidative polymerization. BisEDOT was polymerized electrochemically and its peak anodic oxidation potential, E_{pa} was observed at 0.71 V (see ESI†). Polymerization was also achieved by exposing bisEDOT-SMA thin films to bromine vapours (Fig. 7). The thickness of the films was approx. 50 nm. As a reference, we also polymerized neat bisEDOT thin films (of 15 nm in thickness) in the same way. Bromine was chosen because it is a volatile liquid that readily enters the gas phase and has a sufficient oxidation potential (1.066 V).[36] This approach was adopted from Gleason *et al.* who prepared thin films of PEDOT by exposing EDOT to various oxidants in the gas phase. This process is known as oxidative chemical vapour deposition (oCVD).[37,38] When applied to SMA, oCVD occurs in domains of the precursor already present on the surface of a substrate.

After exposure to the oxidant, the thin films were placed in a vacuum oven at 60 °C for one hour to ensure the removal of any excess bromine. UV-vis spectra of poly(bisEDOT) thin films (Fig. 8a and b) show a significant difference compared to the spectrum of bisEDOT (Fig. 3) which has a λ_{max} of 385 nm. After polymerization neat poly(bisEDOT) absorbs with a λ_{max} of 580 nm while SMA–poly(bisEDOT) has a λ_{max} of 595 nm. This difference could be explained by the periodic confinement of poly(bisEDOT) within the BCP chaperon.

To facilitate C-AFM measurements it was necessary to remove the insulating BCP matrix. After polymerization, the BCP was selectively removed by washing the sample in chloroform while templated poly(bisEDOT) remained on the surface. Neat poly(bisEDOT) thin films required no further treatment. Fig. 8c and d is a comparison of the $I - V$ curves obtained for both neat poly(bisEDOT) and the templated-poly(bisEDOT) thin films.

One goal of this work was to show that using precursors to functional materials to form SMA can be beneficial because the precursor can later be converted into its functional form. The *I–V* curve obtained for the templated poly(bisEDOT) is proof that the *in situ* oxidative polymerization occurs within bisEDOT-SMA thin films and effectively converts the bisEDOT monomer to its electroconductive polymer. Qualitatively, both *I–V* curves exhibit similar behaviour. They show a strong non-Ohmic response to the applied bias and the curves are asymmetric. These features are consistent with that of semiconducting organic polymers.[39] While both curves have similar shapes, quantitatively they are different. Templated poly(bisEDOT) exhibits lower threshold voltages than neat poly(bisEDOT).

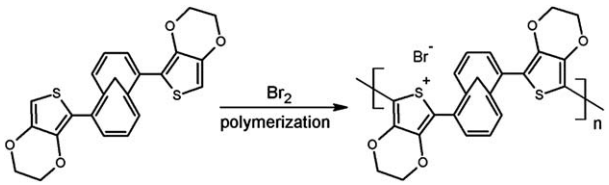

Fig. 7 Oxidative polymerization of bisEDOT using bromine.

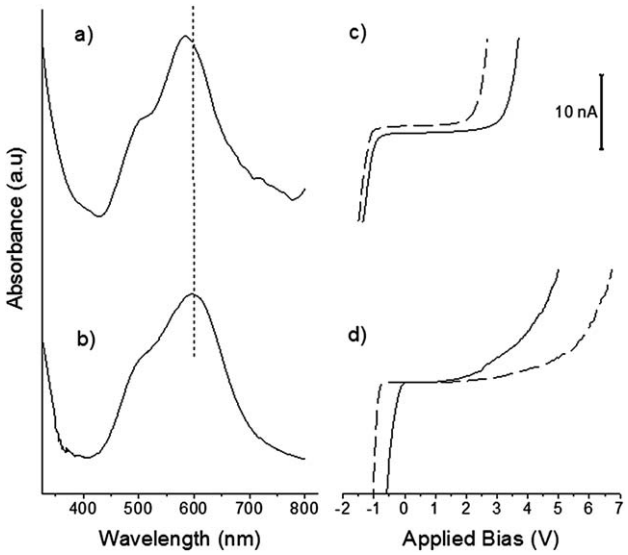

Fig. 8 UV-vis spectra and *I–V* curves comparing poly(bisEDOT) and templated poly(bisEDOT). The spectrum of a poly(bisEDOT) thin film (a) and templated poly(bisEDOT) (b). The *I–V* curve of a poly(bisEDOT) thin film (c) and templated poly(bisEDOT) prepared from its SMA thin film (d). Solid and dashed lines in each *I–V* curve represent the forward or backward scan of voltage applied to the sample, respectively.

Fig. 9 is an AFM topography image of a bisEDOT-SMA thin film after *in situ* polymerization. It clearly reveals minor changes in the morphology of the SMA film upon polymerization. Although the periodicity remains the same (approx. 27 nm), the domains of poly(bisEDOT) appear slightly elevated (approx. 1.0–1.5 nm) above the matrix of PS. We explain it by a re-arrangement of molecules of bisEDOT during polymerization. The polymerization is inhomogeneous across the surface as it can be seen from flat regions. Further investigation and

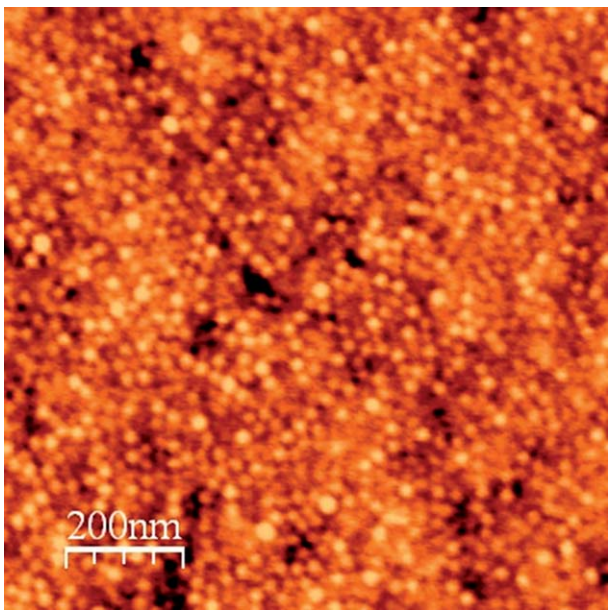

Fig. 9 A 1 × 1 μm AFM topography image of a bisEDOT-SMA thin film after *in situ* polymerization. The thickness of the film is 30 nm.

optimization of the bisEDOT *in situ* polymerization conditions are ongoing.

Yet another problem to be solved is an efficient and reproducible way for selective extraction of the template. Our attempts to remove the template by washing the sample with a selective solvent good for the matrix has led to poor pattern fidelity. After removal of the supporting BCP matrix, the insoluble particles of poly(bisEDOT) remain on the sample surface. However, their size and location do not reproduce the parameters of the SMA template. We speculate that it is caused by low adhesion of poly(bisEDOT) to the substrate.

Conclusions

We report on a new approach for the preparation of electroconductive polymers using a non-hydrogen bonded functional SMA. The polymerization of bisEDOT proceeds within the BCP domains when bisEDOT-SMA thin films are exposed to an oxidant. Characterization of templated poly(bisEDOT) thin films using C-AFM confirms the viability of our approach. We have also discussed the synthesis of this unique molecule which offers many valuable properties due its careful design. Most importantly its interactions with P4VP facilitate SMA formation. This novel SMA between PS-*b*-P4VP and bisEDOT belongs to a new class of SMAs that utilize a combination of weak intermolecular forces other than hydrogen bonds. Another advantage of bisEDOT is that it acts as a fluorescent marker. For the first time evidence of SMA formation was observed in the solution using PL spectroscopy. Further investigation of the properties of conductive polymers synthesized using this SMA method is under way. The authors will be delighted to consider possibilities of collaboration with experts in the field of physics of electroconductive polymers and oCVD to continue research in this area.

Acknowledgements

This work was funded by the National Science Foundation (DMR 0947897) and in part by the Center for Drug Design and Delivery (KISK grant of the Department of Community and Economic Development, Commonwealth of Pennsylvania) and KISK grant C000048830. JDT acknowledges support from the National Science Foundation (DMR-0644727). He also thanks Benjamin C. Streifel (Tovar lab, JHU) for synthetic assistance to prepare the bis(EDOT) annulene monomers used in this study. AS thanks Dr A. Zvelindovsky (University of Central Lancashire, UK) and Dr L. Tsarkova (RWTH Aachen University, Germany) for stimulating discussions.

Notes and references

1 F. S. Bates and G. H. Fredrickson, *Annu. Rev. Phys. Chem.*, 1990, **41**, 525–557.
2 M. W. Matsen and F. S. Bates, *Macromolecules*, 1996, **29**, 1091–1098.
3 I. W. Hamley, *The Physics of Block Copolymers*, Oxford Science Publications, 1998.
4 J. Ruokolainen, R. Makinen, M. Torkkeli, T. Makela, R. Serimaa, G. ten Brinke and O. Ikkala, *Science*, 1998, **280**, 557–560.
5 A. Sidorenko, I. Tokarev, S. Minko and M. Stamm, *J. Am. Chem. Soc.*, 2003, **125**, 12211–12216.
6 I. Tokarev, R. Krenek, Y. Burkov, D. Schmeisser, A. Sidorenko, S. Minko and M. Stamm, *Macromolecules*, 2005, **38**, 507–516.
7 S. Bondzic, J. de Wit, E. Polushkin, A. J. Schouten, G. ten Brinke, J. Ruokolainen, O. Ikkala, I. Dolbnya and W. Bras, *Macromolecules*, 2004, **37**, 9517–9524.
8 E. Polushkin, S. Bondzic, J. de Wit, G. A. van Ekenstein, I. Dolbnya, W. Bras, O. Ikkala and G. ten Brinke, *Macromolecules*, 2005, **38**, 1804–1813.
9 B. K. Kuila, E. B. Gowd and M. Stamm, *Macromolecules*, 2010, **43**, 7713–7721.
10 J. Tata, D. Scalarone, M. Lazzari and O. Chiantore, *Eur. Polym. J.*, 2009, **45**, 2520–2528.
11 A. T. Rodriguez, X. Li, J. Wang, W. A. Steen and H. Fan, *Adv. Funct. Mater.*, 2007, **17**, 2710–2716.
12 A. Laforgue, C. G. Bazuin and R. E. Prud'homme, *Macromolecules*, 2006, **39**, 6473–6482.
13 B. J. Rancatore, C. E. Mauldin, S.-H. Tung, C. Wang, A. Hexemer, J. Strzalka, J. M. J. Frechet and T. Xu, *ACS Nano*, 2010, **4**, 2721–2729.
14 U. Jeong, H. C. Kim, R. L. Rodriguez, I. Y. Tsai, C. M. Stafford, J. K. Kim, C. J. Hawker and T. P. Russell, *Adv. Mater.*, 2002, **14**, 274–276.
15 J. Ruokolainen, M. Saariaho, O. Ikkala, G. ten Brinke, E. L. Thomas, M. Torkkeli and R. Serimaa, *Macromolecules*, 1999, **32**, 1152–1158.
16 A. W. Fahmi, Ph.D. dissertation, Technische Univerität Dresden, 2003.
17 A. W. Fahmi, H. G. Braun and M. Stamm, *Adv. Mater.*, 2003, **15**, 1201.
18 J. Chai, D. Wang, X. Fan and J. M. Buriak, *Nat. Nanotechnol.*, 2007, **2**, 500–506.
19 G. Dennler, M. C. Scharber and C. J. Brabec, *Adv. Mater.*, 2009, **21**, 1323–1338.
20 S. Kirchmeyer and K. Reuter, *J. Mater. Chem.*, 2005, **15**, 2077–2088.
21 B. K. Kuila, B. Nandan, M. Bohme, A. Janke and M. Stamm, *Chem. Commun.*, 2009, 5749–5751.
22 D. Hagaman, T. P. Enright and A. Sidorenko, *Macromolecules*, 2012, **45**, 275–282.
23 E. Vogel and H. D. Roth, *Angew. Chem., Int. Ed. Engl.*, 1964, **3**, 228–229.
24 P. A. Peart, L. M. Repka and J. D. Tovar, *Eur. J. Org. Chem.*, 2008, **2008**, 2193–2206.
25 I. Horcas, R. Fernandez, J. M. Gomez-Rodriguez, J. Colchero, J. Gomez-Herrero and A. M. Baro, *Rev. Sci. Instrum.*, 2007, **78**, 013705.
26 E. Vogel, W. A. Böll and M. Biskup, *Tetrahedron Lett.*, 1966, 1569.
27 T. Pinault, F. Cherioux, B. Therrien and G. Suss-Fink, *Heteroat. Chem.*, 2004, **15**, 121.
28 G. A. Sotzing, J. R. Reynolds and P. J. Steel, *Chem. Mater.*, 1996, **8**, 882.

29 P. A. Peart and J. D. Tovar, *Org. Lett.*, 2007, **9**, 3041.
30 P. A. Peart and J. D. Tovar, *Macromolecules*, 2009, **42**, 4449.
31 E. G. McRae and M. Kasha, *J. Chem. Phys.*, 1958, **28**, 721–722.
32 S. Dante, R. Advincula, C. W. Frank and P. Stroeve, *Langmuir*, 1999, **15**, 193–201.
33 J. Ruokolainen, G. ten Brinke, O. Ikkala, M. Torkkeli and R. Serimaa, *Macromolecules*, 1996, **29**, 3409–3415.
34 J. N. L. Albert, T. D. Bogart, R. L. Lewis, K. L. Beers, M. J. Fasolka, J. B. Hutchison, B. D. Vogt and T. H. Epps III, *Nano Lett.*, 2011, **11**, 1351–1357.
35 S. O'Driscoll, G. Demirel, R. A. Farrell, T. G. Fitzgerald, C. O'Mahony, J. D. Holmes and M. A. Morris, *Polym. Adv. Technol.*, 2001, **22**, 915–923.
36 *Handbook of Chemistry and Physics*, ed. P. Vanysek, 2007.
37 J. P. Lock, S. G. Im and K. K. Gleason, *Macromolecules*, 2006, **39**, 5326–5329.
38 H. Chelawat, S. Vaddiraju and K. Gleason, *Chem. Mater.*, 2010, **22**, 2864–2868.
39 J. C. Bolsée, W. D. Oosterbaan, L. Lutsen, D. Vanderzande and J. Manca, *Org. Electron.*, 2011, **12**, 2084–2089.

